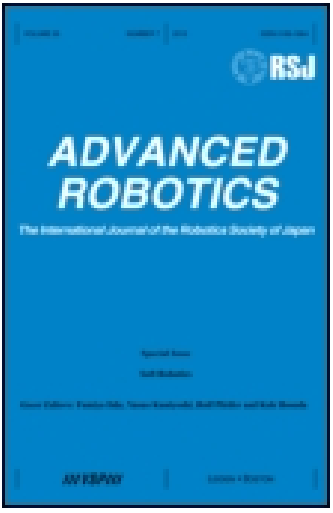

Advanced Robotics
Publication details, including instructions for authors and subscription information:
http://www.tandfonline.com/loi/tadr20

Implementation of omnidirectional crawl for a quadruped robot

Xuedong Chen [a] , Keigo Watanabe [b] , Kazuo Kiguchi [c] & Kiyotaka Izumi [d]

[a] Faculty of Engineering Systems and Technology, Graduate School of Science and Engineering, Saga University

[b] Department of Advanced Systems Control Engineering, Graduate School of Science and Engineering, Saga University

[c] Department of Advanced Systems Control Engineering, Graduate School of Science and Engineering, Saga University

[d] Department of Mechanical Engineering, Faculty of Science and Engineering, Saga University

Published online: 02 Apr 2012.

To cite this article: Xuedong Chen , Keigo Watanabe , Kazuo Kiguchi & Kiyotaka Izumi (2001) Implementation of omnidirectional crawl for a quadruped robot , Advanced Robotics, 15:2, 169-190, DOI: 10.1163/15685530152116218

To link to this article: http://dx.doi.org/10.1163/15685530152116218

Advanced Robotics, Vol. 15, No. 2, pp. 169–190 (2001)

Full paper

Implementation of omnidirectional crawl for a quadruped robot

XUEDONG CHEN [1], KEIGO WATANABE [2,*], KAZUO KIGUCHI [3] and KIYOTAKA IZUMI [4]

[1] *Faculty of Engineering Systems and Technology, Graduate School of Science and Engineering, Saga University, 1 Honjomachi, Saga 840-8502, Japan*
[2] *Department of Advanced Systems Control Engineering, Graduate School of Science and Engineering, Saga University, 1 Honjomachi, Saga 840-8502, Japan*
[3] *Department of Advanced Systems Control Engineering, Graduate School of Science and Engineering, Saga University, 1 Honjomachi, Saga 840-8502, Japan*
[4] *Department of Mechanical Engineering, Faculty of Science and Engineering, Saga University, 1 Honjomachi, Saga 840-8502, Japan*

Received 20 April 2000; accepted 22 July 2000

Abstract—As a reptile animal crawls in a cluttered environment, so a quadruped robot should be able to crawl on an irregular ground profile with its static stability by adopting the straight-going and standstill-turning free gaits. The generalized and explicit formulations for the automatic generation of straight-going gaits and various standstill-turning gaits are presented in this paper. The maximized stride for the straight-going gait and the maximum turning angle for the turning gait of a quadruped robot named TITAN-VIII in a gait cycle are discussed by considering the robot's mechanism constraints and the irregularities of the ground profile. The control algorithm, including control of the joint positions of the robot, is described to implement the desired walking path of the quadruped robot. The effectiveness of the proposed method is demonstrated through experimental result.

Keywords: Quadruped robot; omnidirectional crawl; gait generation; gait control; straight-going gait; standstill-turning gait.

1. INTRODUCTION

It is a well-known fact that considerable enthusiasm has built up among researchers in legged robots, mainly due to their superior flexibility on irregular surfaces over wheeled robots. As one type of legged vehicles, quadruped robots should be able to crawl on rough ground like a four-legged animal does on the ground. Moreover,

*To whom correspondence should be addressed. E-mail: watanabe@me.saga-u.ac.jp

if there are some obstacles such as convex terrain that cannot be stepped on/over and concave terrain that cannot be crossed over, the robots should be able to avoid them. Therefore, a quadruped robot must be controlled in such a way that it possesses omnidirectional mobility. However, implementation of omnidirectional crawl depends on the generation and control of the appropriate gait composed of the sequence of swing leg, the footstep and the forward direction of the robot, etc.

There are two main types of gaits adopted in walking by a quadruped robot: periodic and non-periodic. A periodic gait implies that the feet are lifted and placed with a fixed pattern. A quadruped robot with a periodic gait can be easily controlled and it can move with an optimal stability margin. However, it should be noted that periodic gaits can only be used on relatively flat terrain. So-called non-periodic gaits are regarded as 'free' gaits in the sense that a fixed pattern for lifting and placing feet is not required. Several algorithms for free gait generation have been developed in the past [1–15]. For example, Hirose *et al.* [2, 15] introduced the diagonal principle to generate a free gait for a quadruped robot. Pal *et al.* [4] used a heuristic graph search algorithm in generating a straight-line gait for a quadruped robot. Recently, Bai *et al.* [1] presented a method of free gait generation for quadrupeds by introducing the primary/secondary gait. Chen *et al.* [9] described the study on motion planning of a walking robot using ordinal optimization. Celaya *et al.* [10] considered a control structure for the locomotion of a legged robot on a difficult terrain. It should be noted, however, that they suggested, but seldom implemented or tested in practice, the algorithms for the gait generation or the gait control of the quadruped robots, and the proposed algorithms had their limitations. Also, it is very difficult or complicated to position robots in real-time in complex environments for on-line walking control with navigation, because of the complexity of the gait implementation. Apart from that, Kimura *et al.* [16] and Sano *et al.* [17] implemented straight-line walking of quadruped robots by using a neural oscillator and a discrete-time model, respectively. Hugel *et al.* [18] presented the implementation of an efficient walking pattern for quadruped robots without considering the rough ground profile. In addition, Hirose *et al.* [19] elaborated the algorithm to generate the continuous and straight trajectory of the center-of-gravity of a quadruped walking vehicle by introducing a concept of gait control named dynamic and static fusion gait. Moreover, they performed intermittent trot gait of a quadruped walking machine [20]. Here, we extend our previous works [21, 22] to derive the generalized and explicit formulation for the generation and control of the various gaits, and to implement the omnidirectional crawl of a quadruped robot named TITAN-VIII by using the proposed control algorithm.

On the other hand, it is observed that a four-legged animal always crawls on the ground with some regularities in its sequence of the swing leg and its footstep, unless it needs to change its forward direction for obstacle avoidance. A quadruped robot with omnidirectional mobility can walk from a current point to any target point by adopting a crab-like gait without changing body direction or the combination of the standstill-turning gait about the current point and the straight-going gait. As

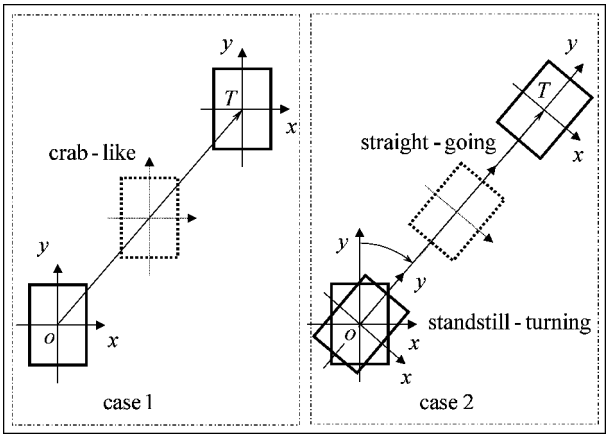

Figure 1. A quadruped robot crawls from the current point o to a desired target T by using the crab-like gait (case 1) or the standstill-turning and straight-going gait (case 2).

shown in Fig. 1, for example, the robot can crawl from the current point o to a desired target T by using the crab-like gait (case 1) or the standstill-turning and straight-going gait (case 2). The crab-like crawl defined as the translational gait has been developed for TITAN-VIII in our previous work [23]. Here, we discuss the straight-going gait and standstill-turning gait for the omnidirectional crawl of the robot. Since the quadruped robot can lift or place its foot to a certain height or depth, the robot is able to adopt such gaits to walk on the rough ground as a four-leg animal does. So-called obstacles defined in this paper denote those which the robot cannot step on/over or cross over, unlike those presented in references [1, 9, 10, 24]. When the robot runs across such an obstacle, it can use proper gaits for obstacle avoidance. Therefore, the key to the question is how to generate and control the gaits so that the desired crawl path can be implemented for a quadruped robot in a cluttered environment.

In this paper, we address the gait generation and control for the quadruped robot TITAN-VIII. Note, however that, the duty factor β [7] of the proposed gaits is kept at its lowest value of 0.75 to obtain a high crawl speed. The rest of the paper is organized as follows. Section 2 presents the generation of various gaits. The biggest stride for the straight-going gait and the maximum turning angle for the standstill-turning gait of the robot in a gait cycle are also discussed in this section. Section 3 focuses on the control of the gait. The experimental result is shown in Section 4. Finally, Section 5 discusses some of the conclusions drawn from this research.

2. GENERATION OF GAIT

Figure 2 shows the basic mechanism of the quadruped robot TITAN-VIII. A_i ($i = 1, 2, 3, 4$) denotes the ith foot of the robot. Σ_c ($c-xyz$) denotes the frame fixed at the robot body and c is the center-of-gravity of the robot. Σ_o ($o-XYZ$) is the

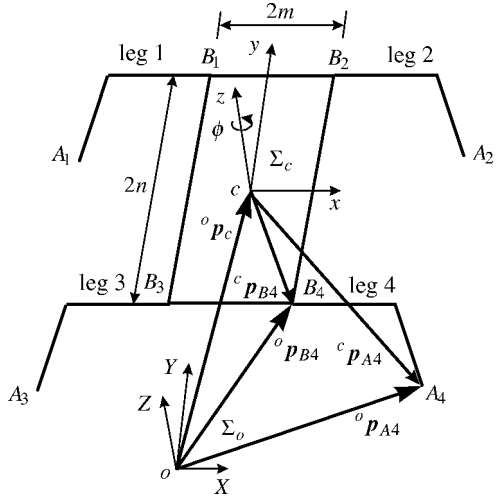

Figure 2. The basic mechanism of the quadruped robot TITAN-VIII.

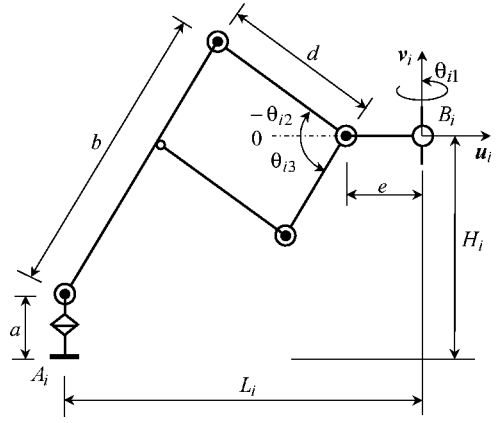

Figure 3. The equivalent leg mechanism of TITAN-VIII.

reference coordinate frame, whose $X-Y$ plane is fixed to the ground. The equivalent leg mechanism of TITAN-VIII is shown in Fig. 3. There are three actuated joints in each leg, whose variables are denoted by θ_{i1}, θ_{i2} and θ_{i3}, respectively. a, b, d and e are the lengths of the links, respectively. It is obvious that, the performance of lift and placement of the ith leg depends on controlling θ_{i2} and θ_{i3} whereas the performance of swing of the ith leg is related in actuating θ_{i1}.

We define a successive performance (*lift up–swing ahead–put down*) for every leg of the quadruped robot as a gait cycle. Moreover, the initial posture of the quadruped robot is given by the status of $\theta_{i1} = 0$ for $i = 1, 2, 3$ and 4. Note that, at the initial posture, θ_{i2} and θ_{i3} for $i = 1, 2, 3$ and 4 have to be controlled in such a way that every leg can stand on the rough ground profile. Once it has performed a gait cycle, irrespective of the straight-going gait or turning gait, the quadruped

robot returns to the initial posture for the next gait cycle. Therefore, the robot can realize the natural and smooth transition from the current gait cycle to the successive one. In our previous work [21], an approach to the analysis of the static stability was presented for the quadruped robot by defining the statically stable area (SSA) for the foothold. See Appendix for the definition of SSA. The proposed approach is applied to generate the free gait based on the static stability. Assume the frame Σ_c is parallel to the frame Σ_o in the initial posture of the robot. According to the analysis of the mechanism constraints of TITAN-VIII [25], it is shown that the robot can omnidirectionally crawl on the ground as long as the robot's body is parallel to the surfaces with which the robot's feet contact, even if the ground profile is irregular or sloping. Therefore, the $x-y$ plane in Σ_c is kept being parallel to the $X-Y$ plane in Σ_o when the robot crawls on the rough ground profile. Here, the formulations for the generation of the straight-going gait and the standstill-turning gait are presented as follows.

2.1. Generation of the straight-going gait

The straight-going gait discussed here possesses the regular sequence of the swing leg with equal footstep of every leg, but without a fixed pattern of the legs' lift and placement in a gait cycle because of the irregular ground profile, as with a four-legged animal's crawl on the rough ground. Adjusting the robot footstep can change the stride of the robot in every gait cycle (every step). The forward direction of the quadruped robot is along the line of the y-axis in Σ_c.

2.1.1. The sequence of the swing leg. Since the duty factor is equal to 0.75, the quadruped robot must only adopt three legs to support its body at any time; the robot's body has to keep a continuous movement in a gait cycle, and the robot's body takes a movement of a quarter of the footstep for every leg working as the swing leg. Therefore, the sequence for the swing leg should be selected in such a way that the quadruped robot is stable at an arbitrary moment. Figure 4a shows the quadruped robot in the initial posture, i.e. as shown in Fig. 3, $\theta_{i1} = 0$, and L_i is equal to the initial value denoted by L_0, while H_i is subjected to the height of the robot's center-of-gravity and the rough ground profile, for $i = 1, 2, 3$ and 4. The initial position vector of the center-of-gravity in Σ_o is given as:

$$ {}^{o}\rho_c = \left[{}^{o}x_c \;\; {}^{o}y_c \;\; {}^{o}z_c\right]^T. \tag{1} $$

Thus, the position vectors of every foothold in Σ_o can be expressed by:

$$ {}^{o}\rho_{A1} = \left[{}^{o}x_c - L_0 - m \quad {}^{o}y_c + n \quad {}^{o}z_{a1}\right]^T, \tag{2} $$

$$ {}^{o}\rho_{A2} = \left[{}^{o}x_c + L_0 + m \quad {}^{o}y_c + n \quad {}^{o}z_{a2}\right]^T, \tag{3} $$

$$ {}^{o}\rho_{A3} = \left[{}^{o}x_c - L_0 - m \quad {}^{o}y_c - n \quad {}^{o}z_{a3}\right]^T, \tag{4} $$

$$ {}^{o}\rho_{A4} = \left[{}^{o}x_c + L_0 + m \quad {}^{o}y_c - n \quad {}^{o}z_{a4}\right]^T, \tag{5} $$

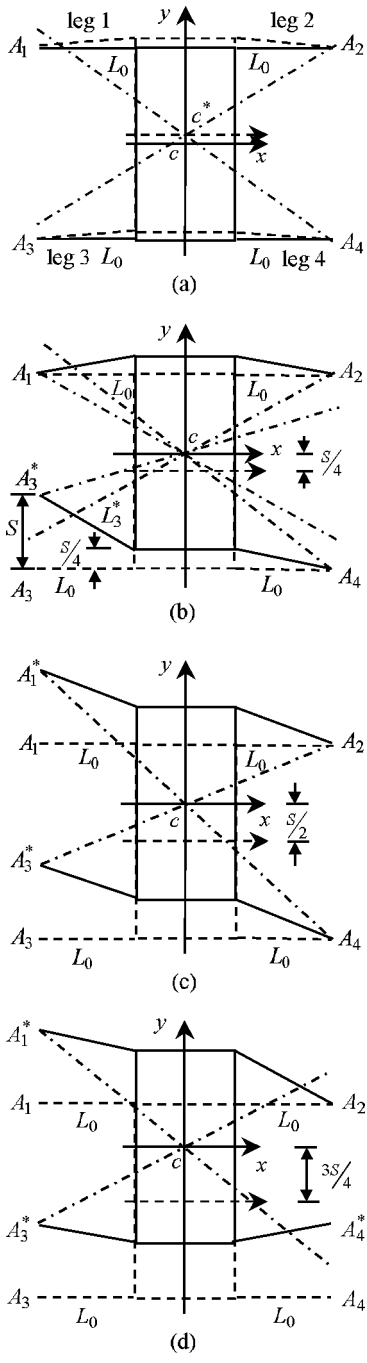

Figure 4. The posture variation of the robot in the straight-going gait.

where ${}^{o}z_{ai}$ $(i = 1, 2, 3, 4)$ is the initial height of the ith leg's foothold. At this moment the stable area for the first and third feet is the region limited by the boundary lines cA_1 and cA_3. Once the robot begins to crawl forward, the stable area is varied, e.g. when the robot's center-of-gravity moves to c^*, the stable area for the first and third feet is presented as the shaded region in Fig. 4a. Clearly, the third leg can be first selected as the swing leg, whereas the first leg cannot, owing to the fact that the third foot is beyond the stable area. While the third leg takes a footstep forward as the swing leg, the center-of-gravity moves ahead a quarter of the footstep denoted by S. The posture of the robot is varied as shown in Fig. 4b, thus, ${}^{o}\rho_c$ and ${}^{o}\rho_{A3}$ become:

$$ {}^{o}\rho_c = \begin{bmatrix} {}^{o}x_c & {}^{o}y_c + S/4 & {}^{o}z_c + \Delta h/4 \end{bmatrix}^T, \tag{6} $$

$$ {}^{o}\rho_{A3} = \begin{bmatrix} {}^{o}x_c - L_0 - m & {}^{o}y_c - n + S & {}^{o}z^*_{a3} \end{bmatrix}^T, \tag{7} $$

where ${}^{o}z^*_{a3}$ is the next height of the third leg's foothold in the gait cycle and Δh denotes the change in the height of the center-of-gravity in the gait cycle. Generally, $\Delta h = 0$, except when the robot crawls on stairs, etc. In Fig. 4b, the shaded area to the right of the y-axis denotes the stable area for the second and fourth feet, while the shaded area to the left of the y-axis is the stable area for the first and third feet. It is obvious that only the first leg can be selected as the next swing leg after the third leg. Figure 4c shows the posture of the robot after taking a footstep of the first leg. ${}^{o}\rho_c$ and ${}^{o}\rho_{A1}$ are varied as follows:

$$ {}^{o}\rho_c = \begin{bmatrix} {}^{o}x_c & {}^{o}y_c + S/2 & {}^{o}z_c + \Delta h/2 \end{bmatrix}^T, \tag{8} $$

$$ {}^{o}\rho_{A1} = \begin{bmatrix} {}^{o}x_c - L_0 - m & {}^{o}y_c + n + S & {}^{o}z^*_{a1} \end{bmatrix}^T, \tag{9} $$

where ${}^{o}z^*_{a1}$ is the next height of the first leg's foothold in the gait cycle. Similar to the selection of the first swing leg, the fourth leg should be the next swing leg after the third and first legs. Once the fourth leg has finished the role as a swing leg, the robot's posture is as Fig. 4d. The position vectors of the center-of-gravity and the fourth leg's foothold are expressed by:

$$ {}^{o}\rho_c = \begin{bmatrix} {}^{o}x_c & {}^{o}y_c + 3S/4 & {}^{o}z_c + 3\Delta h/4 \end{bmatrix}^T, \tag{10} $$

$$ {}^{o}\rho_{A4} = \begin{bmatrix} {}^{o}x_c + L_0 + m & {}^{o}y_c + n + S & {}^{o}z^*_{a4} \end{bmatrix}^T, \tag{11} $$

where ${}^{o}z^*_{a4}$ is the next height of the fourth leg's foothold in the gait cycle. Finally, the second leg makes a step forward and then the robot returns to the initial posture for the next gait cycle. At this moment, it follows that:

$$ {}^{o}\rho_c = \begin{bmatrix} {}^{o}x_c & {}^{o}y_c + S & {}^{o}z_c + \Delta h \end{bmatrix}^T, \tag{12} $$

$$ {}^{o}\rho_{A2} = \begin{bmatrix} {}^{o}x_c + L_0 + m & {}^{o}y_c + n + S & {}^{o}z^*_{a2} \end{bmatrix}^T, \tag{13} $$

where ${}^{o}z^*_{a2}$ is the next height of the second leg's foothold in the gait cycle.

Similarly, the sequence of swing leg can also be determined as $4 \rightarrow 2 \rightarrow 3 \rightarrow 1$. It should be noted that the stride of the robot can be adjusted by giving different S.

2.1.2. The maximized stride. The maximized stride, denoted by $S_{\max}$, is defined as the longest footstep of a quadruped robot in a gait cycle, which is subjected to the robot's mechanism constraints and the roughness of the ground profile. Conventionally, a maximum stride in the current state will not always bring wider strides in the following steps. In some cases, especially, a smaller stride in the first step contributes to a wider stride in the second and after steps [26, 27]. According to the present straight-going gait definition as above, we know that the robot movement (stride) is equal to the footstep of legs in a gait cycle, but there is no assurance of four legs being equally stretched in the gait cycle. When the maximum stretch of four legs reaches the allowance, the robot takes a maximized stride. Therefore, the robot stride is limited by the maximum stretch of four legs in a gait cycle. In addition, since the robot always returns to its initial posture after a gait cycle, it can independently obtain a maximized stride in every gait cycle. Figure 5 shows the allowance of leg stretch of TITAN-VIII, in which the dotted line presents the case of flat terrain while the solid line denotes the case of rough terrain. Define $L_{i\max}$ as the allowance stretch of the ith leg in the horizontal. For the case of flat terrain, it follows that:

$$L_{i\max} = \sqrt{(b+d)^2 - (H_0 - a)^2} + e, \tag{14}$$

where H_0 is the height of the robot center-of-gravity in the initial posture. To obtain a valid and possible bigger stretch in the horizontal, considering the roughness of the ground profile and the change in the robot height in the gait cycle, equation (14)

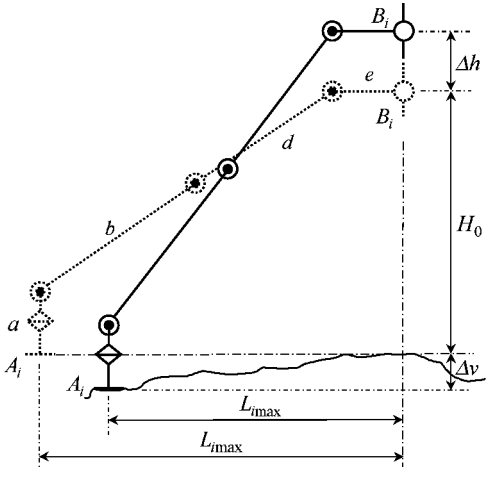

Figure 5. The allowance of leg stretch of TITAN-VIII.

becomes:

$$L_{i\max} = \sqrt{(b+d)^2 - (H_0 + \Delta h + \Delta v - a)^2} + e, \tag{15}$$

where Δv denotes the roughness of the ground profile to which the robot can adapt itself. From Fig. 4, we easily know that the robot stretches the third and second legs further than the others in a gait cycle when it is crawling on a terrain with a certain roughness. In Fig. 4b or d, the stretched length of the third or the second legs in the horizontal can be expressed by:

$$L_i^* = \sqrt{L_0^2 + (3S/4)^2}, \tag{16}$$

for $i = 2$ or 3. Therefore, we have:

$$\sqrt{L_0^2 + (3S_{\max}/4)^2} = L_{i\max}. \tag{17}$$

It follows that:

$$S_{\max} = \frac{4}{3}\sqrt{L_{i\max}^2 - L_0^2}. \tag{18}$$

Hence, the stride of the quadruped robot S should satisfy:

$$S \leqslant S_{\max}. \tag{19}$$

2.2. Generation of the standstill-turning gait

In order to achieve great mobility of the robot, we devise the standstill-turning gaits about the geometric center of the robot. Assume the turning angle ϕ abides by the right-hand rule, i.e. if the robot takes a left turning then $\phi > 0$; otherwise, $\phi \leqslant 0$. The determination of the sequence of the swing leg and the maximum turning angle in a gait cycle is presented below.

2.2.1. The sequence of the swing leg. First, the formulation of the next footholds for every leg of the quadruped robot in a gait cycle can be derived. As shown in Fig. 6a, the initial posture of the robot is presented by the solid line and the robot returns to the next initial posture drawn by the dotted line after standstill-turning with turning angle ϕ about the robot center c. At this moment, the orientation matrix of Σ_c with respect to Σ_o is obtained as:

$${}^o\boldsymbol{R}_c = \begin{bmatrix} \cos\phi & -\sin\phi & 0 \\ \sin\phi & \cos\phi & 0 \\ 0 & 0 & 1 \end{bmatrix}. \tag{20}$$

According to the relationship:

$${}^o\rho_{Ai} = {}^o\rho_c + {}^o\boldsymbol{R}_c{}^c\rho_{Ai}, \tag{21}$$

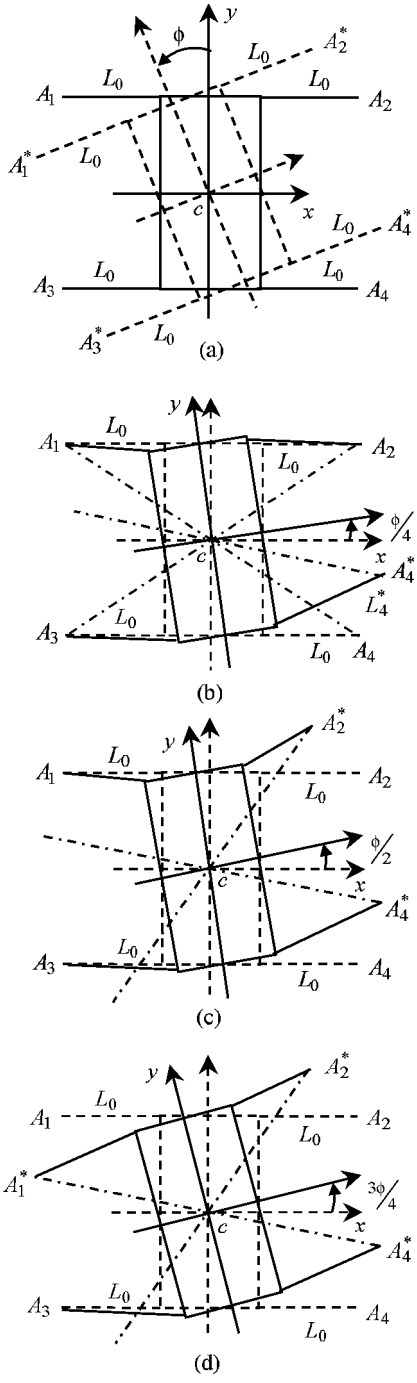

Figure 6. The posture variation of the robot in the left turning gait.

we can obtain the position vectors of the next footholds of four legs in the gait cycle as follows:

$$ {}^{o}\rho_{A1} = \left[{}^{o}x_c - (L_0 + m)\cos\phi - n\sin\phi \quad {}^{o}y_c - (L_0 + m)\sin\phi + n\cos\phi \quad {}^{o}z^*_{a1} \right]^T, \tag{22} $$

$$ {}^{o}\rho_{A2} = \left[{}^{o}x_c + (L_0 + m)\cos\phi - n\sin\phi \quad {}^{o}y_c + (L_0 + m)\sin\phi + n\cos\phi \quad {}^{o}z^*_{a2} \right]^T, \tag{23} $$

$$ {}^{o}\rho_{A3} = \left[{}^{o}x_c - (L_0 + m)\cos\phi + n\sin\phi \quad {}^{o}y_c - (L_0 + m)\sin\phi - n\cos\phi \quad {}^{o}z^*_{a3} \right]^T, \tag{24} $$

$$ {}^{o}\rho_{A4} = \left[{}^{o}x_c + (L_0 + m)\cos\phi + n\sin\phi \quad {}^{o}y_c + (L_0 + m)\sin\phi - n\cos\phi \quad {}^{o}z^*_{a4} \right]^T, \tag{25} $$

where ${}^{o}z^*_{ai}$ $(i = 1, 2, 3, 4)$ denotes the next height of the ith leg's foothold in the gait cycle, which depends on the profile of the rough ground.

Similar to the analysis process of the straight-going gait, the sequence of the swing leg of a left standstill-turning gait is briefly described as follows. The fourth leg can be selected as the first swing leg. As shown in Fig. 6b, the second leg should be the next swing leg. After the fourth and second legs, only the first leg can be selected as the next swing leg as shown in Fig. 6c. Finally, the third leg takes a footstep from the position as Fig. 6d, then the robot returns to the initial posture drawn by the dotted line in Fig. 6a. Therefore, the sequence of swing leg for left turning is $4 \rightarrow 2 \rightarrow 1 \rightarrow 3$.

Similarly, the sequence of the swing leg of a right standstill-turning gait about the robot center c can be determined as $3 \rightarrow 1 \rightarrow 2 \rightarrow 4$ or $2 \rightarrow 4 \rightarrow 3 \rightarrow 1$.

2.2.2. Maximum turning angle. Due to the mechanism constraints and the irregularities of the ground profile, the turning angle of the quadruped robot is limited in a gait cycle. The maximum turning angle of the robot in a gait cycle is denoted by $\phi_{\max}$. From Fig. 6, we can easily find that the third and fourth legs are stretched further than the first and second legs, when the robot takes a left turning. In Fig. 6b, the fourth leg will take its longest stretch in the horizontal L^*_4 in a gait cycle, if the robot achieves a left turning gait with the maximum turning angle $\phi_{\max}$. Thus, we obtain:

$$ L^*_4 = \sqrt{({}^{o}x_{a4} - {}^{o}x_{b4})^2 + ({}^{o}y_{a4} - {}^{o}y_{b4})^2}, \tag{26} $$

where ${}^{o}x_{a4}$ and ${}^{o}y_{a4}$ are known from equation (25) with $\phi = \phi_{\max}$, while ${}^{o}x_{b4}$ and ${}^{o}y_{b4}$ can be obtained from the following relationship:

$$ {}^{o}\rho_{Bi} = {}^{o}\rho_c + {}^{o}\boldsymbol{R}_c {}^{c}\rho_{Bi}, \tag{27} $$

where ${}^{o}\rho_{Bi}$ is a constant. Then, it follows that:

$$ {}^{o}x_{b4} = {}^{o}x_c + m\cos\frac{\phi_{\max}}{4} + n\sin\frac{\phi_{\max}}{4}, \tag{28} $$

$$ {}^{o}y_{b4} = {}^{o}y_c + m\sin\frac{\phi_{\max}}{4} - n\cos\frac{\phi_{\max}}{4}. \tag{29} $$

Consequently, we have:

$$ L_4^* = \sqrt{f_1\sin\frac{3\phi_{\max}}{4} - f_2\cos\frac{3\phi_{\max}}{4} + f_3}, \tag{30} $$

where f_1, f_2 and f_3 are the constants which are to be the functions of L_0, m and n. Therefore, the maximum turning angle $\phi_{\max}$ must be subjected to:

$$ \sqrt{f_1\sin\frac{3\phi_{\max}}{4} - f_2\cos\frac{3\phi_{\max}}{4} + f_3} = L_{i\max}, \tag{31} $$

where $L_{i\max}$ is the same as above. Note that according to the geometric symmetry of the robot, equation (31) is also applied to the right turning gait of the robot.

2.3. Foot trajectory of the swing leg

The generation of the foot trajectory of the swing leg is very important because the quadruped robot adapts itself to the rough ground profile by means of the adaptability of every swing leg to the ground profile in lift and placement. The step height of the swing leg at arbitrary time t is denoted by $h_{ai}(t)$ during the process of *lift up–swing ahead–put down* corresponding to the time interval of $t_0 \leqslant t \leqslant t_0 + T/4$, where t_0 denotes the starting time of the ith leg performed as the swing leg and T denotes the period of a gait cycle.

In order to adapt the swing leg to the rough ground profile, the changeable footstep and the various directions, irrespective of straight-going or turning gait, the foot trajectory should be modeled by two cases:

Case I: For the case of ${}^{o}z_{ai}^* \geqslant {}^{o}z_{ai}$, where ${}^{o}z_{ai}$ and ${}^{o}z_{ai}^*$ denote the heights of the previous foothold and the next foothold of the ith leg in a gait cycle, respectively, the step height of the swing leg is given by:

$$ h_{ai}(t) = \begin{cases} {}^{o}z_{ai} + \Delta v(1 - \mathrm{e}^{\delta(t_0 - t)}) & t_0 \leqslant t < t_0 + T/4 \\ {}^{o}z_{ai}^* & t = t_0 + T/4, \end{cases} \tag{32} $$

where Δv is the roughness of the ground profile and δ is a constant ($1 < \delta < 10$). The foot trajectory of the swing leg is shown in Fig. 7a.

Case II: For the case of ${}^{o}z_{ai}^* < {}^{o}z_{ai}$, it must be that:

$$ h_{ai}(t) = {}^{o}z_{ai} + ({}^{o}z_{ai} - {}^{o}z_{ai}^*)\left(1 - \left|\frac{t_0 + \Delta t_0 - t}{\Delta t_0}\right|\right)/\varepsilon, \tag{33} $$

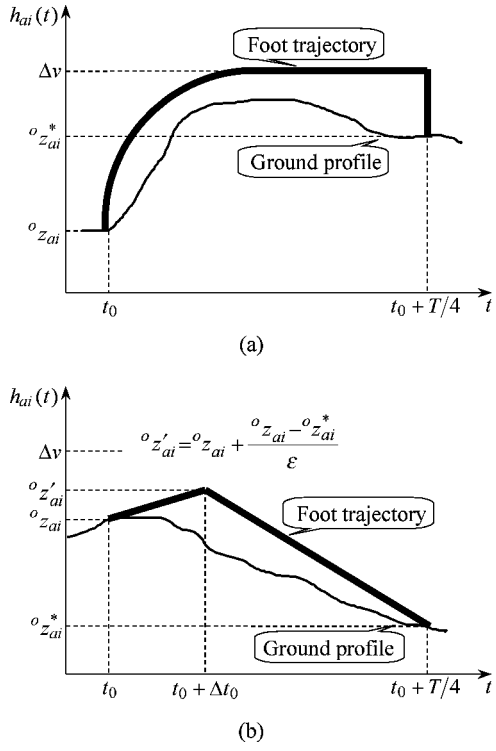

Figure 7. The foot trajectories of the swing leg.

for $t_0 \leqslant t \leqslant t_0 + T/4$, where $\Delta t_0 = T/16$ and $\varepsilon = 2$, or $\Delta t_0 = T/24$ and $\varepsilon = 4$, etc. The foot trajectory of the swing leg is shown in Fig. 7b.

3. GAIT CONTROL

Based on the desired gait generated above, the position vectors of the robot's center-of-gravity and every foothold can be known at an arbitrary moment in a gait cycle. Now, the key problem for the implementation of the desired crawl is how to control the joint positions of the robot.

3.1. Control of the joint positions

Here, we propose a generalized formulation for the determination of the joint positions when the quadruped robot is crawling in the straight-going or turning gait. From Fig. 3, we have:

$$\overrightarrow{A_i B_i} = L_i \boldsymbol{u}_i + H_i \boldsymbol{v}_i, \tag{34}$$

where $\overrightarrow{A_i B_i}$ denotes the vector from A_i to B_i, and $\boldsymbol{u}_i$ and $\boldsymbol{v}_i$ are the unit vectors perpendicular to and coincident with the axis of the revolute joint B_i, respectively,

and:

$$\begin{cases} L_i = b\cos\theta_{i3} + d\cos\theta_{i2} + e \\ H_i = b\sin\theta_{i3} + d\sin\theta_{i2} + a. \end{cases} \tag{35}$$

As shown in Figs 2 and 3, the axes of four revolute joints of B_i ($i = 1, 2, 3, 4$) are perpendicular to the robot body, i.e. $\boldsymbol{v}_i$, for $i = 1, 2, 3$ and 4, are parallel to the z-axis of Σ_c. Therefore, equation (34) is also tenable in Σ_c. We thus obtain:

$$^{c}\rho_{Bi} - {}^{c}\rho_{Ai} = L_i\boldsymbol{u}_i + H_i\boldsymbol{v}_i. \tag{36}$$

Let $^{c}\boldsymbol{E}_i = {}^{c}\rho_{Bi} - {}^{c}\rho_{Ai} = [{}^{c}e_{ix}\,{}^{c}e_{iy}\,{}^{c}e_{iz}]^T$, which is known from the desired gait. Moreover, from equation (21) we have:

$$^{c}\rho_{Ai} = {}^{o}\boldsymbol{R}_c^{-1}\,{}^{o}\rho_{Ai} - {}^{o}\boldsymbol{R}_c^{-1}\,{}^{o}\rho_c. \tag{37}$$

Note that the orientation matrix $^{o}\boldsymbol{R}_c$ is orthogonal so that $^{o}\boldsymbol{R}_c^{-1} = {}^{o}\boldsymbol{R}_c^{T}$. Therefore, we obtain

$$^{c}\boldsymbol{E}_i = {}^{c}\rho_{Bi} + {}^{o}\boldsymbol{R}_c^{T}\,{}^{o}\rho_c - {}^{o}\boldsymbol{R}_c^{T}\,{}^{o}\rho_{Ai}, \tag{38}$$

where $^{c}\rho_{Bi}$, for $i = 1, 2, 3$ and 4, are constants resulting from the robot mechanism, $^{o}\boldsymbol{R}_c$ and $^{o}\rho_{Ai}$, for $i = 1, 2, 3$ and 4, are known from the desired gait at an arbitrary moment in a gait cycle. Thus, equation (36) becomes:

$$L_i\boldsymbol{u}_i + H_i\boldsymbol{v}_i = {}^{c}\rho_{Bi} + {}^{o}\boldsymbol{R}_c^{T}\,{}^{o}\rho_c - {}^{o}\boldsymbol{R}_c^{T}\,{}^{o}\rho_{Ai}. \tag{39}$$

Therefore, we finally obtain:

$$\begin{cases} b\cos\theta_{i3} + d\cos\theta_{i2} = \sqrt{{}^{c}e_{ix}^2 + {}^{c}e_{iy}^2} \\ b\sin\theta_{i3} + d\sin\theta_{i2} = {}^{c}e_{iz} \\ \tan\theta_{i1} = {}^{c}e_{iy}/{}^{c}e_{ix}. \end{cases} \tag{40}$$

Solving equation (40), we can obtain the joint positions θ_{i1}, θ_{i2} and θ_{i3}, for $i = 1$, 2, 3 and 4, of the quadruped robot.

3.2. Structure of the control algorithm

Following the above result, the quadruped robot can be controlled to crawl on the rough ground profile with the automatic generation of a gait composed of the sequence of swing leg, stride and foot trajectory of the swing leg. For simplicity of control, the roughness of the ground profile Δv is given a conservative value by considering the robot's mechanism constraints. The rough ground may be considered to be 'flat' ground if the roughness of the ground profile is less than the conservative value, whereas the terrain whose roughness is larger than the conservative value is regarded as an obstacle for the quadruped robot. Therefore, the stride of the quadruped robot, S, is taken as $S_{\max}$ with Δv which is equal to the conservative value in the corresponding equations.

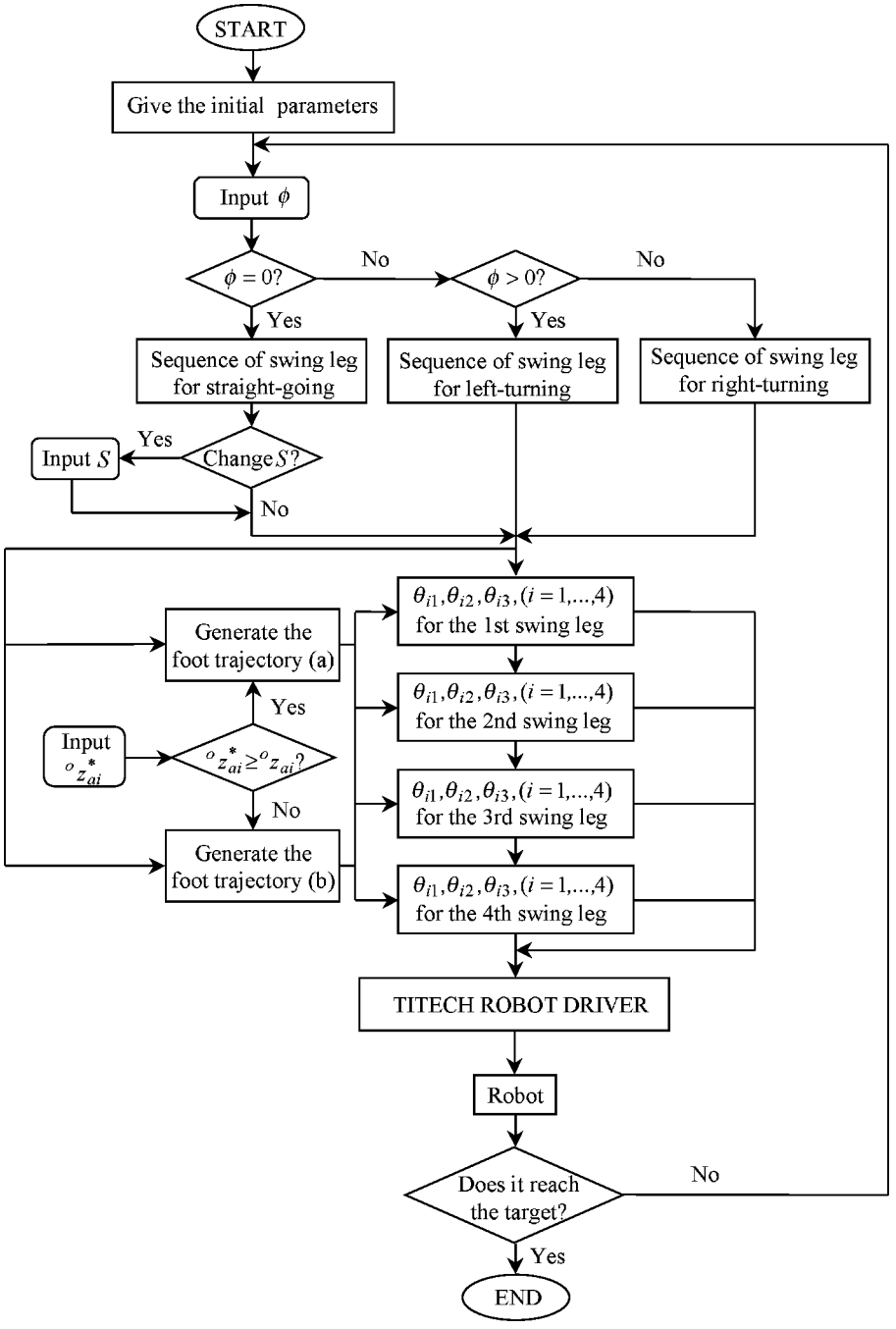

Figure 8. The structure of the control algorithm.

Figure 8 shows the basic structure of the proposed control algorithm. The initial posture parameters of TITAN-VIII and the conservative roughness of ground profile are given as the initial inputs to the control system. Once the desired turning angle ϕ and the change of the robot's height Δh in a gait cycle are given as the inputs, the control system can automatically generate the corresponding swing leg sequence. Due to the different swing leg sequence in a gait cycle, three modules have to be allocated to the straight-going gait with $\phi = 0$, the left standstill-turning gait with $\phi > 0$ and the right standstill-turning gait with $\phi < 0$, respectively. If needed, moreover, the stride of the robot can be adjusted in every gait cycle. A gait cycle of the quadruped robot is divided into four sections corresponding to each swing leg. The foot trajectory of each swing leg can be generated automatically based on the given ${}^{o}z^{*}_{ai}$. The joint positions of the robot are sequentially determined to meet the needs of the desired gait. Finally, the quadruped robot is actuated through the TITECH ROBOT DRIVER at every sampling interval.

4. EXPERIMENT RESULT

The structure size of TITAN-VIII is as follows [mm]: $m = 101$, $n = 201$, $a = 43$, $b = 200$, $d = 155$ and $e = 45$. The initial position of a leg is given by the status with $\theta_{i1} = 0$, $\theta_{i2} = 0$ and $\theta_{i3} = 75$ deg, so that $L_0 = 252$ mm and $H_0 = 236$ mm. Give the conservative roughness of the ground profile as $\Delta v = 50$ mm. The robot crawls without changing the height of its center-of-gravity, i.e. $\Delta h = 0$. According to equations (18) and (31), the biggest stride and the maximum turning angle in a

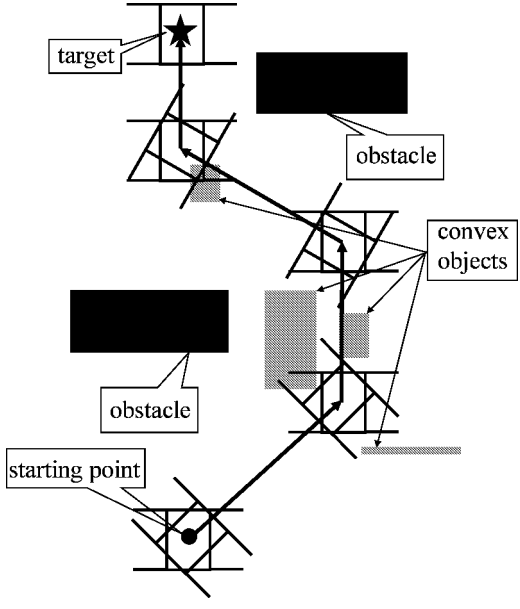

Figure 9. The desired path of TITAV-VIII in the experiment.

gait cycle can be evaluated as $S_{\max} = 226$ mm and $\phi_{\max} = \pm 44$ deg, respectively. In addition, take a gait cycle every 4.8 s and a sampling every 20 ms.

The experiment was conducted in our laboratory. There were some obstacles that the robot could not step on/over and some convex objects that the robot could step on/over on the terrain adopted in the experiment. The terrain and the desired crawl path of the robot TITAN-VIII are presented in Fig. 9. Using the control system proposed in this paper, TITAN-VIII could be actuated to crawl to the specified

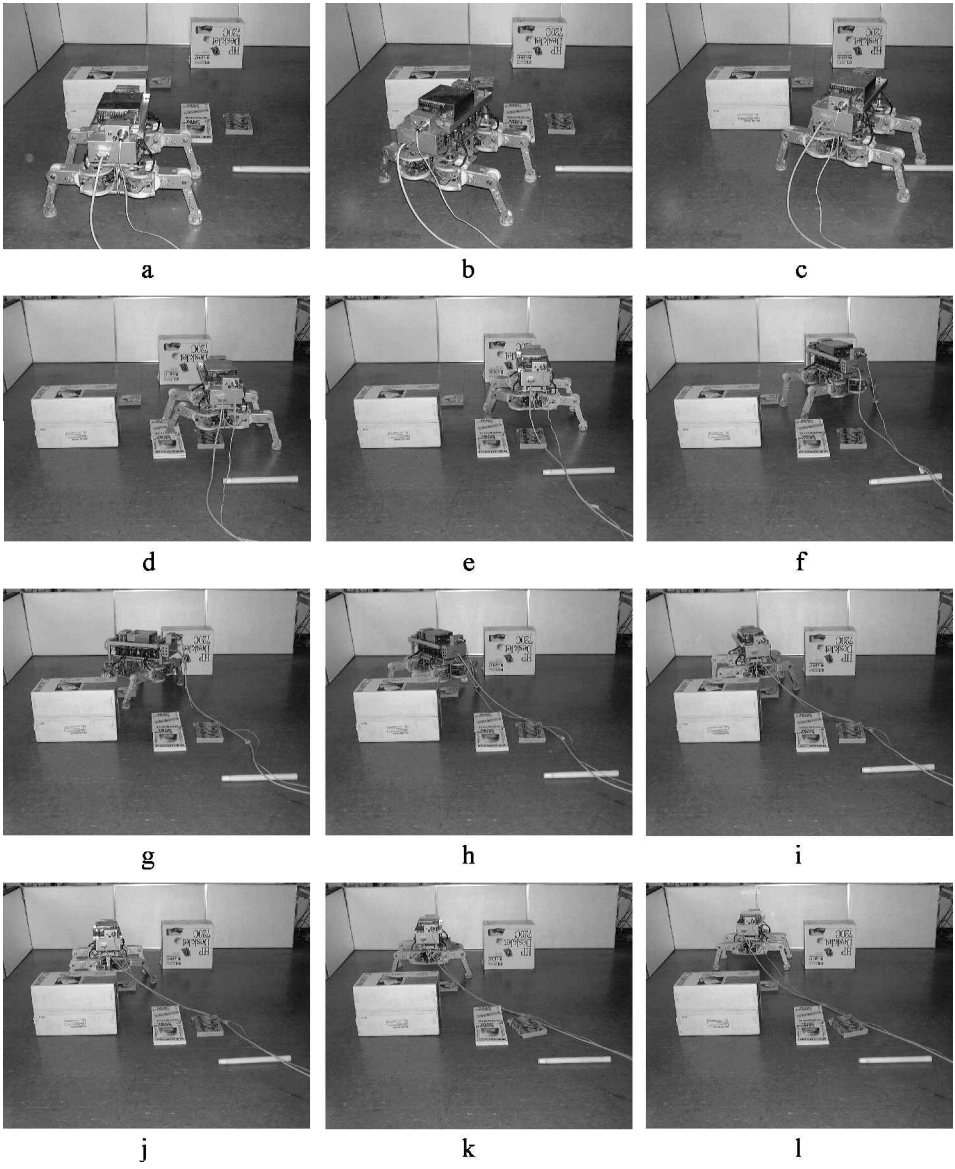

Figure 10. The pictures of the experimental result of TITAN-VIII.

target with the desired path. The experimental result is shown in Fig. 10. During the walking process, the robot avoided two obstacles, stepping over some objects as well as stepping on some convex objects which were considered as the parts of the rough ground.

5. CONCLUSIONS

In this paper, we have described the method for generating a straight-going gait and a standstill-turning gait for a quadruped robot crawling on rough ground. The formulations of evaluating the maximized stride and the maximum turning angle have been derived for the straight-going gait and the turning gait in a gait cycle, respectively. The approach to determining the joint positions of the robot has also been developed for the implementation of the desired gait. In brief, the systematic formulation for the implementation of omnidirectional crawl has been proposed for the quadruped robot TITAN-VIII. In addition to the concise and explicit physical meaning of gait definition, and the simplicity and ease of implementation, the proposed free gait has the following superior performance, compared to the conventional gait. First, the robot can realize a natural and smooth transition from one gait cycle to a successive one, because the robot returns to the initial posture after each gait cycle whenever it is a straight-going or a standstill-turning gait. Next, a valid and possible large stride of the robot can be obtained in every gait cycle by considering various factors such as mechanism constraints, uneven terrain, change in the robot status, etc. Moreover, it is easy to position and control the robot in a complex environment for autonomous walking by invoking sensor-based navigation. The effectiveness of the proposed approach has been illustrated by experimental results. It should be also pointed out that the proposed method can be applied to general crawing with different duty factors and discrete body motions, provided that the control algorithm is adjusted correspondingly.

REFERENCES

1. S. Bai, K. H. Low, G. Seet and T. Zielinska, A new free gait generation for quadrupeds based on primary/secondary gait, in: *Proc. IEEE Int. Conf. Robotics and Automation*, Detroit, Michigan, pp. 1371–1376 (1999).
2. S. Hirose, H. Iwasaki and Y. Umetani, The basic study of the intelligent gait control for quadrupedal walking vehicle, *Trans. Soc. Instrument Control Eng.* **18** (2), 193–200 (1982) (in Japanese).
3. J. Pan and J. Cheng, Study on quadruped walking robot climbing and walking down slope, in: *Proc. IEEE/RSJ Int. Workshop on Intelligent Robots and Systems*, Osaka, Japan, pp. 1531–1534 (1991).
4. P. K. Pal and K. Jayarajan, Generation of free gait — a graph search approach, *IEEE Trans. Robotics Automat.* **7** (3), 299–305 (1991).

5. Z. Bien, M. G. Chun and H. S. Son, An optimal turning gait for a quadruped walking robot, in: *Proc. IEEE/RSJ Int. Workshop on Intelligent Robots and System*, Osaka, Japan, pp. 1511–1517 (1991).
6. D. J. Pack and H. S. Kang, An omnidirectional gait control using a graph search method for a quadruped walking robot, in: *Proc. IEEE Int. Conf. Robotics and Automation*, Nagoya, Japan, pp. 988–993 (1995).
7. K. Inagaki and H. Kobayashi, A gait transition for quadruped walking machine, in: *Proc. IEEE/RSJ Int. Conf. on Intelligent Robots and Systems*, Yokohama, Japan, pp. 525–531 (1993).
8. T. Omata and E. Tanaka, A quadruped robot which can take various postures, in: *Proc. IEEE Int. Conf. Robotics and Automation*, Detroit, Michigan, pp. 2366–2371 (1999).
9. C. H. Chen, V. Kumar and Y. C. Luo, Motion planning of walking robots using ordinal optimization, *IEEE Robotics Automat. Mag.* **5** (2), 22–32 (1998).
10. E. Celaya and J. M. Porta, A control structure for the locomotion of a legged robot on difficult terrain, *IEEE Robotics Automat. Mag.* **5** (2), 43–51 (1998).
11. R. M. Alexander, Gaits of mammals and turtles, *J. Robotics Soc. Jpn* **11** (3), 314–319 (1993).
12. C. Villard, P. Gorce and J. G. Fontaine, Study of a distributed control architecture for a quadruped robot, *J. Intelligent Robotic Syst.* **11** (3), 269–291 (1995).
13. K. Akimoto, S. Watanabe and M. Yano, An insect robot controlled by emergence of gait patterns, in: *Proc. 3rd Int. Symp. on Artificial Life and Robotics*, Oita, Japan, pp. 110–113 (1998).
14. R. Prajoux and F. Martins, A walk supervisor architecture for autonomous four-legged robots embedding real-time decision-making, in: *Proc. IEEE/RSJ Int. Conf. on Intelligent Robots and Systems*, Osaka, Japan, pp. 200–207 (1996).
15. S. Hirose and O. Kunieda, Generalized standard leg trajectory for quadruped walking vehicle, *Trans. Soc. Instrument Control Eng.* **25** (4), 455–461 (1989) (in Japanese).
16. H. Kimura, S. Akiyama and K. Sakurama, Dynamic walking on irregular terrain and running on flat terrain of the quadruped using neural oscillator, *J. Robotics Soc. Jpn* **16** (8), 1138–1145 (1998) (in Japanese).
17. A. Sano, J. Furusho and S. Ozeki, A pace gait of quadruped robot based on the control of walking cycle using a discrete-time model, *J. Robotics Soc. Jpn* **9** (7), 865–876 (1991) (in Japanese).
18. V. Hugel and P. Blazevic, Towards efficient implementation of quadruped gaits with duty factor of 0.75, in: *Proc. 1999 IEEE Int. Conf. Robotics and Automation*, Detroit, Michigan, pp. 2360–2365 (1999).
19. S. Hirose and K. Yoneda, Dynamic and static fusion control and continuous trajectory generation of quadruped walking vehicle, *J. Robotics Soc. Jpn* **9** (3), 267–275 (1991) (in Japanese).
20. K. Yoneda, H. Iiyama and S. Hirose, Intermittent trot gait of a quadruped walking machine — dynamic stability control of an omnidirectional walk, *J. Robotics Soc. Jpn* **14** (6), 881–886 (1996) (in Japanese).
21. X. D. Chen, K. Watanabe and K. Izumi, A new method on judgment of static stability for the quadruped robot, in: *Proc. IEEE Int. Conf. on Systems, Man and Cybernetics*, Tokyo, Japan, Vol. 4, pp. 953–958 (1999).
22. X. D. Chen, K. Watanabe and K. Izumi, Joint positions and robot stability of the omnidirectional crawling quadruped robot, *J. Robotics Mechatron.* **11** (6), 510–517 (1999).
23. X. D. Chen, K. Watanabe and K. Izumi, Study on control algorithm of translational crawl for a quadruped robot, in: *Proc. IEEE Int. Conf. on Systems, Man and Cybernetics*, Tokyo, Japan, Vol. IV, pp. 959–964 (1999).
24. H. Tsukagoshi, T. Doi and S. Hirose, A gait for quadruped walking robots to step over obstacles by means of a visual sensor, in: *Proc. 16th Ann. Conf. of the Robotics Society of Japan*, Tokyo, Japan, pp. 541–542 (1998) (in Japanese).
25. X. D. Chen, K. Watanabe and K. Izumi, Kinematic solution of a quadruped walking robot — posture analysis of TITAN-VIII, in: *Proc. 14th IFAC World Congr.*, Bejing, China, Vol. B, pp. 343–348 (1999).

26. S. Hirose, H. Kikuchi and Y. Umetani, The standard circular gait of the quadruped walking vehicle, *J. Robotics Soc. Jpn* **2** (6), 545–556 (1984) (in Japanese).
27. S. Hirose, Y. Fukuda and H. Kikuchi, Control system of quadruped walking vehicle, *J. Robotics Soc. Jpn* **3** (4), 304–323 (1985) (in Japanese).

APPENDIX: DEFINITION OF THE SSA

Figure A.1 shows the vertical view of the quadruped robot in the world coordinate frame Σ_o. A_i, A_j, A_k and A_l denote the four feet of the robot, respectively. A_i^*, A_j^*, A_k^*, A_l^* and c^* are the projections of A_i, A_j, A_k, A_l and c in the horizontal plane, i.e. $X-Y$ plane of Σ_o, respectively. Assume ***Line ic***, ***Line jc***, ***Line kc*** and ***Line lc*** are the straight lines through both of A_i^* and c^*, A_j^* and c^*, A_k^* and c^* and A_l^* and c^* in the $X-Y$ plane, respectively. We define these lines as the boundary lines. The shade area in Fig. A.1 is limited by the boundary lines of ***Line ic*** and ***Line jc***. Clearly, it can be understood that, irrespective of the attitude of the robot body, as long as one point of both A_k^* and A_l^* lies inside of the shaded area the quadruped robot is supported by three legs corresponding to A_i^*, A_j^* and one such point, respectively. The reason is that the triangle composed of A_i^*, A_j^* and the arbitrary point in the shaded area surely surrounds c^*, whereas it is not true if such arbitrary point is beyond the shaded area. Here, the shaded area is regarded as the SSA for the footholds of A_k and A_l. Every two boundary lines construct such an area for the corresponding footholds. The following information can be obtained through the SSA: if the robot is statically stable or not, the leg to be selected as the next swing leg and the allowed range of static stability.

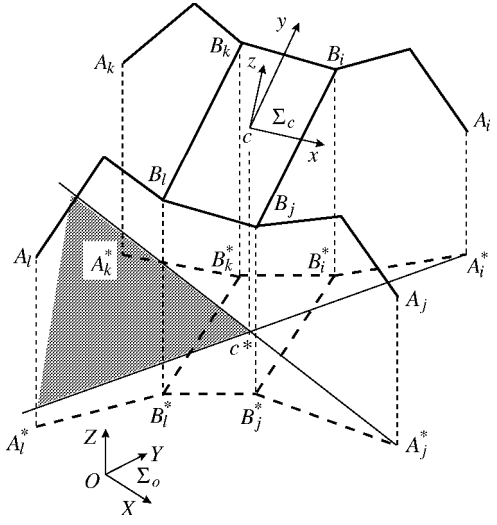

Figure A.1. Definition of the SSA.

ABOUT THE AUTHORS

Xuedong Chen received the Bachelor of Engineering degree in mechanical engineering from Wuhan University of Technology, China in 1984, the Master of Engineering degree in mechanical engineering from WUT, China in 1989. Currently he is working towards the PhD degree in the Faculty of Engineering Systems and Technology, Graduate School of Science and Engineering, Saga University, Japan. He was an assistant with the Department of Mechanical Engineering, WUT, China between 1984–1986. He worked as an assistant professor in the Department of Mechanical Engineering, WUT, China between 1989–1996. From 1996 to 1997, he was an associate professor in the Department of Mechanical Engineering, WUT, China. His research interests include robotics, dynamics, intelligent robots and applications of soft computing for robot control.

Keigo Watanabe received BE and ME degrees in Mechanical Engineering from the University of Tokushima in 1976 and 1978, respectively, and a DE degree in Aeronautical Engineering from Kyushu University in 1984. From 1980 to March 1985, he was a Research Associate in Kyushu University. From April 1985 to March 1990, he was an Associate Professor in the College of Engineering, Shizuoka University. From April 1990 to March 1993 he was an Associate Professor, and from April 1993 to March 1998 he was a full Professor in the Department of Mechanical Engineering, Saga University. From April 1998, he is now with the Department of Advanced Systems Control Engineering, Graduate School of Science and Engineering, Saga University. His research interests are in stochastic adaptive estimation and control, robust control, neural network control, fuzzy control, genetic algorithms and their applications to the robotic control. He has published more than 250 technical papers and is author or editor of 14 books, including *Adaptive Estimation and Control* (Prentice Hall), *Stochastic Large-Scale Engineering Systems* (Marcel Dekker) and *Intelligent Control Based on Flexible Neural Networks* (Kluwer). He is an active reviewer of many journals or transactions, an editor-in-chief of *Machine Intelligence and Robotic Control*, and editorial board members of the *Journal of Intelligent and Robotic Systems* and the *Journal of Knowledge-Based Intelligent Engineering Systems*. He is a member of the Society of Instrument and Control Engineers, the Japan Society of Mechanical Engineers, the Japan Society for Precision Engineering, the Institute of Systems, Control and Information Engineers, the Japan Society for Aeronautical and Space Sciences, the Robotics Society of Japan, Japan Society for Fuzzy Theory and Systems, and IEEE.

Kazuo Kiguchi received the Bachelor of Engineering degree in mechanical engineering from Niigata University, Japan in 1986, the Master of Applied Science degree in Mechanical Engineering from University of Ottawa, Canada in 1993, and the Doctor of Engineering degree in Mechano-Informatics and Systems from Nagoya University, Japan in 1997. He was a research Engineer with Mazda Motor Co. between 1989–1991, and with MHI Aerospace Systems Co. between 1989–1991. He worked for the Department of Industrial and Systems Engineering, Niigata College of Technology, Japan between 1994–1999. He is currently an associate professor in the Department of Science and Engineering, Saga University. He recieved the J. F. Engelberger Best Paper Award at WAC2000. His research interests include biorobotics, intelligent robots, machine learning, applications of soft computing for robot control, and application of robotics for medicine. He is a member of the Robotics Society of Japan, the Society of Instrument and Control Engineers, the Japan Society of Mechanical Engineers, Japan Society of Fuzzy Theory and Systems, IEEE, and International Neural Networks Society.

Kiyotaka Izumi recieved a BE degree in Electrical Engineering from the Nagasaki Institute of Applied Science in 1991, an ME degree in Electrical Engineering from the Saga University in 1993, and a DE degree from the Division of Engineering Systems and Technology of Saga University in 1996. From April in 1996, he is a Research Associate in the Department of Mechanical Engineering at Saga University. His research interests are in robust control, fuzzy control, behavior based control, genetic algorithms, evolutionary strategy and their applications to mobile robotic control. He is a member of the Society of Intrument and Control Engineers, the Japan Society of Mechanical Engineers, the Robotics Society of Japan, Japan Society for Fuzzy Theory and Systems, the Institute of Electronics, Information and Communication Engineers, and the Japan Society for Precision Engineering.